

# MHD Squeezing Flow of Casson Nanofluid with Chemical Reaction, Thermal Radiation and Heat Generation/Absorption

Open  
Access

Nur Azlina Mat Noor<sup>1</sup>, Sharidan Shafie<sup>1</sup>, Mohd Ariff Admon<sup>1,\*</sup>

<sup>1</sup> Department of Mathematical Sciences, Faculty of Science, Universiti Teknologi Malaysia, 81310 Johor Bahru, Johor, Malaysia

## ARTICLE INFO

## ABSTRACT

### Article history:

Received 17 December 2019

Received in revised form 23 January 2020

Accepted 23 January 2020

Available online 30 March 2020

The heat and mass transfer characteristics on unsteady squeezing flow of magnetohydrodynamic (MHD) Casson nanofluid with chemical reaction, thermal radiation and heat generation/absorption effects is investigated in this study. The influences of viscous and joule dissipation are also examined. The flow is caused by squeezing between two parallel plates embedded in a porous medium. The highly coupled nonlinear partial differential equations are reduced to a system of nonlinear ordinary differential equations via similarity transformations. The transformed equations are solved using numerical scheme of Keller-box method. The accuracy of present method is validated through comparison of skin friction coefficient, Nusselt and Sherwood numbers with previously published results. Comparisons reveal that good agreements are achieved. Graphical results for velocity, temperature and nanoparticles concentration are analysed with various parameters. Findings demonstrate that the fluid velocity and temperature enhance when the plates move closer. Besides, increase in Hartmann number suppressed the fluid velocity and concentration due to the presence of strong Lorentz forces. The Brownian motion boosts the fluid temperature and concentration. Moreover, nanoparticles concentration is found to be higher in constructive chemical reaction and opposite effect is observed in destructive chemical reaction.

### Keywords:

Squeezing flow; Casson nanofluid;  
chemical reaction; thermal radiation;  
heat generation/absorption

Copyright © 2020 PENERBIT AKADEMIA BARU - All rights reserved

## 1. Introduction

Recent advancement in nanotechnology has led to the development of a new innovative class of heat transfer fluids known as nanofluid. Choi and Eastman [11] were the first to introduce the nanofluids engineered by colloidal suspensions of nanometer-sized particles in a base fluid. Conventional heat transfer fluids or base fluids such as water, ethylene glycol or kerosene oil have limited heat transfer capability due to their low thermal conductivity. Thus, the concept of nanofluid was discovered to improve the heat transfer performance by dispersing metallic or non-metallic

\* Corresponding author.

E-mail address: [ariffadmon@utm.my](mailto:ariffadmon@utm.my) (Mohd Ariff Admon)

<https://doi.org/10.37934/arfmts.68.2.94111>

nanoparticles in the conventional fluids [3]. Moreover, Eastman *et al.*, [13] reported that the addition of copper (10 nm) particles in ethylene glycol increases the thermal conductivity up to 40%. Several researchers stated that suspending 1–5% volume of nanoparticles in base fluids can enhance the thermal conductivity by more than 20% [21,39,40]. Later, Buongiorno [7] examined seven slip mechanisms that generate a relative velocity between nanoparticles and base fluids. He concluded that among all the mechanisms, only Brownian diffusion and thermophoresis are found to be important factors in convective flow of nanofluid. Brownian motion and thermophoresis of nanoparticles effectively boost the thermal conductivity of base fluid. Nowadays, Buongiorno's model has been adopted by many researchers in their study [5,14,23,30].

The study of boundary layer flow caused by squeezing between two parallel plates has increased tremendously due to its applications in chemical engineering and food industry. Some practical examples of squeeze flow include compression, polymer processing and injection molding. Stefan [35] initiated the investigation on behavior of a lubricant confined between approaching horizontal surfaces. Later, the study of squeeze film lubrication between two infinitely long parallel plates was introduced by Cameron [8]. The squeeze film phenomenon occurs when two surfaces are separated by a lubricant and moved towards each other with a normal stress. Commonly, the lubricant is a viscous fluid. Wang [38] studied unsteady squeezing flow of an incompressible viscous fluid between two parallel plates. The similar problem was solved by Bujurke *et al.*, [6], Rashidi *et al.*, [27] and Khan *et al.*, [16] via semi-analytical methods.

Casson fluid is a non-Newtonian fluid classified as shear thinning fluid because it exhibits an infinite viscosity at zero velocity gradient, no flow occurs when force is applied below the yield stress, and zero viscosity at infinite velocity gradient. The Casson model was originally invented by Casson (1959) for printing inks and silicon suspension. The model is ideal for studying the flow characteristics of blood. Common examples of Casson fluid are honey, jelly, tomato sauce and concentrated fruit juices [33]. Researches done by Khan *et al.*, [17] and Sampath *et al.*, [28] are among the pioneering works to investigate the unsteady squeezing flow of Casson fluid between two parallel plates.

The squeeze flow of electrically conducting fluids between parallel plates under the influence of magnetic field has been studied extensively in recent years. The unsteady two-dimensional flow of a viscous MHD fluid between two parallel plates was solved by Siddiqui *et al.*, [32] using homotopy perturbation method (HPM). Sweet *et al.*, [36] extended the work of Siddiqui *et al.*, [32] by varying the fluid density to be a model parameter. In non-Newtonian fluid, Ahmed *et al.*, [2] presented the analytical solutions of unsteady MHD squeezing flow of Casson fluid between two parallel plates. A novel algorithm was developed by Al-Saif and Jasim [4] to solve the similar problem of Ahmed *et al.*, [2]. The research of fluid flow through a porous medium in the presence of MHD effect is important in the applications of geothermal energy recovery, oil extraction, nuclear reactors and thermal energy storage. A porous medium is a material that contains fluid-filled pores. Khan *et al.*, [18] analysed MHD flow of Casson fluid squeezing between two parallel plates embedded in porous medium.

The impact of viscous dissipation on heat transfer of nanofluid flow has received great attention due to its engineering applications such as temperature rises in polymer processing, injection molding and high rates extrusion. The viscous dissipation effect is only significant for the fluids with high velocity and viscosity. It is worth mentioning that Tiwari and Das model was recently used by Sheikholeslami and Ganji [29], Pourmehran *et al.*, [26] and Mittal and Pandit [22]. All of them investigated the problem of unsteady flow and heat transfer of a nanofluid squeezing between two parallel plates in the presence of viscous dissipation. They implemented different types of methods in obtaining the solution. The squeezing flow of Copper-water and Copper-kerosene with magnetic field and viscous dissipation effects using Tiwari and Das model was discussed by Acharya *et al.*, [1]

and Çelik [10]. A series of studies on the similar problem had been investigated by Sheikholeslami *et al.*, [30], Hedayati and Ramiar [15] and Azimi and Riazi [5]. They employed Buongiorno's model on their study. Muhammad *et al.*, [23] analysed the effects of MHD and thermal radiation on squeezing nanofluid flow between two parallel plates. Heat and mass transfer characteristics were examined by considering Brownian motion and thermophoresis. The unsteady squeezing flow and heat transfer of nanofluid under the influence of MHD, viscous dissipation and thermal radiation was reported by Dogonchi *et al.*, [12] and Sheikholeslami *et al.*, [31] using Tiwari and Das model and Buongiorno's model, respectively. Madaki *et al.*, [19] studied the unsteady squeezing nanofluid flow with viscous dissipation and thermal radiation effects using Tiwari and Das model. Madaki *et al.*, [20] extended their works by including heat generation or absorption on the flow field. In non-Newtonian fluid, the influence of magnetic field on unsteady squeezing flow of Casson nanofluid between parallel plates in a porous medium was presented by Sobamowo [33]. The analytical solution was obtained via method of matched asymptotic expansion. Later, Sobamowo *et al.*, [34] performed the similar problem by applying two different techniques, differential transformation method and variation of parameters method.

The literature survey discussed above reveals that most of the existing studies on unsteady squeezing flow between two parallel plates are done for viscous fluid. The study involving non-Newtonian fluids, especially Casson nanofluid, has not been given much consideration. Motivated by the limitation of the above references, this study concentrates on the unsteady MHD flow of Casson nanofluid with the effects of chemical reaction, thermal radiation and heat generation or absorption. The fluid flow is generated by squeezing between two parallel plates through a porous medium in the presence of viscous and Joule dissipation. The governing equations are reduced to ordinary differential equations using non dimensional variables. The transformed equations are solved numerically via Keller box method. An algorithm is developed in MATLAB software to compute the numerical solutions and plot the associated graphs. The results for wall shear stress, heat and mass transfer rate are compared with existing literature results to check the accuracy of the present algorithm. The effects of various parameters on the behavior of fluid velocity, temperature and nanoparticles concentration are examined.

## 2. Mathematical Formulation

Consider an unsteady, two dimensional, incompressible MHD flow of Casson nanofluid squeezing between two parallel plates through a porous medium under the influence of chemical reaction, thermal radiation and heat generation/absorption. The viscous and Joule dissipation effects is retained. The physical behavior of this model is studied using the Cartesian coordinate system. The  $x$ -axis is measured along the horizontal direction of the plates and  $y$ -axis is taken normal to the plates. The two plates are separated by a time-dependent distance  $y = \pm l(1 - \alpha t)^{1/2} = \pm h(t)$ . The fluid flow occurs due to the motion of the upper plate at a distance  $h(t) = +l(1 - \alpha t)^{1/2}$  with the velocity of the form  $v_w(t) = \frac{-\alpha l}{2\sqrt{1-\alpha t}}$  towards or away from the stationary lower plate located at  $h(t) = -l(1 - \alpha t)^{1/2}$ . Both plates are squeezed when  $\alpha > 0$  until they reach  $t = 1/\alpha$  and they are separated for  $\alpha < 0$ . The parameter  $\alpha$  is correlated to the dimensions of  $(\text{time})^{-1}$  and  $\alpha t < 1$ . Here,  $\alpha$  is a constant,  $l$  denotes the initial position of the plate (at  $t = 0$ ) and  $t$  is the time throughout the flow. A uniform magnetic field of strength  $B(t) = B_0(1 - \alpha t)^{-1/2}$  is applied perpendicular to the plates with constant  $B_0$ . The flow configurations and coordinate system are presented in Figure 1.

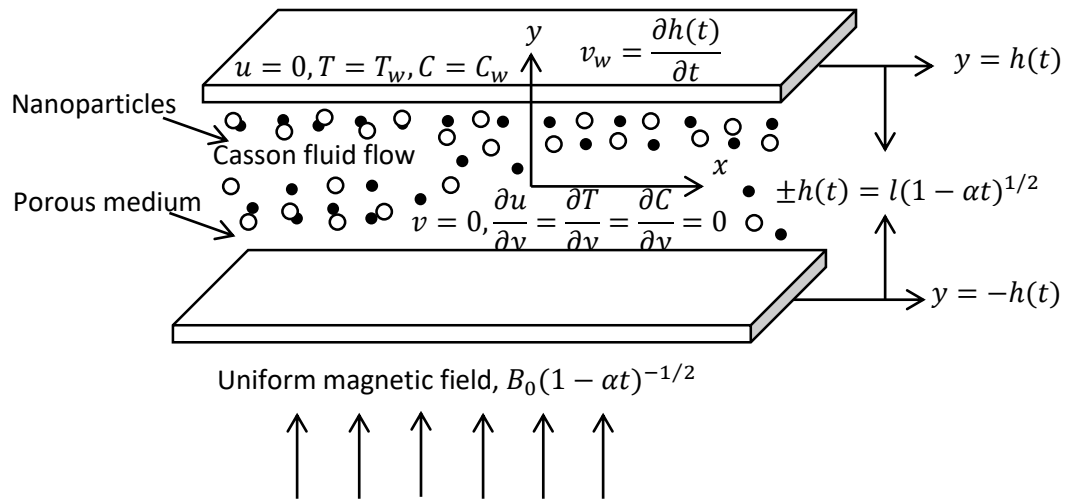


Fig. 1. Physical model and coordinate system

The governing equations of continuity, momentum, energy and concentration for Casson nanofluid using above-mentioned assumptions with boundary layer approximations are given as

$$\frac{\partial u}{\partial x} + \frac{\partial v}{\partial y} = 0 \quad (1)$$

$$\frac{\partial u}{\partial t} + u \frac{\partial u}{\partial x} + v \frac{\partial u}{\partial y} = \nu_f \left(1 + \frac{1}{\beta}\right) \frac{\partial^2 u}{\partial y^2} - \frac{\sigma B^2(t)}{\rho_f} u - \nu_f \left(1 + \frac{1}{\beta}\right) \frac{\varphi}{k_1} u \quad (2)$$

$$\begin{aligned} \frac{\partial T}{\partial t} + u \frac{\partial T}{\partial x} + v \frac{\partial T}{\partial y} = \alpha_f \frac{\partial^2 T}{\partial y^2} + \tau \left[ D_B \frac{\partial C}{\partial y} \frac{\partial T}{\partial y} + \frac{D_T}{T_\infty} \left(\frac{\partial T}{\partial y}\right)^2 \right] + \frac{\nu_f}{c_f} \left(1 + \frac{1}{\beta}\right) \left[ 4 \left(\frac{\partial u}{\partial x}\right)^2 + \left(\frac{\partial u}{\partial y}\right)^2 \right] \\ + \frac{\sigma B^2(t)}{(\rho c)_f} u^2 - \frac{1}{(\rho c)_f} \frac{\partial q_r}{\partial y} + \frac{Q(t)}{(\rho c)_f} (T - T_\infty) \end{aligned} \quad (3)$$

$$\frac{\partial C}{\partial t} + u \frac{\partial C}{\partial x} + v \frac{\partial C}{\partial y} = D_B \frac{\partial^2 C}{\partial y^2} + \frac{D_T}{T_\infty} \frac{\partial^2 T}{\partial y^2} - k_c (C - C_\infty) \quad (4)$$

where  $u$  and  $v$  are the velocity components along the  $x$  and  $y$  directions, respectively,  $\nu_f$  is kinematic viscosity,  $\rho_f$  is the fluid density,  $\sigma$  is the electrical conductivity,  $\beta$  is the Casson parameter,  $\varphi$  is the porosity,  $k_1(t) = k_0(1 - \alpha t)$  is the time dependent permeability of porous medium,  $k_0$  is the permeability constant,  $T$  is the fluid temperature,  $C$  is the nanoparticles concentration,  $\alpha_f = \frac{k}{(\rho c)_f}$  is the thermal diffusivity of the Casson fluid,  $k$  is the thermal conductivity of the Casson fluid,  $c_f$  is the specific heat of fluid,  $\tau = \frac{(\rho c)_p}{(\rho c)_f}$  is the ratio between the heat capacity of the nanoparticles material and heat capacity of the fluid,  $\rho_p$  is the density of nanoparticles,  $c_p$  is the specific heat of nanoparticles,  $D_B$  is the Brownian diffusion coefficient,  $D_T$  is the thermophoretic diffusion coefficient,  $q_r$  is the radiative heat flux,  $Q(t) = \frac{Q_0}{1 - \alpha t}$  is heat generation or absorption coefficient,  $k_c(t) = ak_2(1 - \alpha t)^{-1}$  is the variable rate of chemical reaction,  $k_2$  is the constant reaction rate and  $a$  is the reference length along the fluid flow. The temperature and nanoparticles concentration at free stream are  $T_\infty$  and  $C_\infty$ , respectively. The corresponding boundary conditions are written as follows,

$$u = 0, v = v_w = \frac{\partial h(t)}{\partial t}, T = T_w, C = C_w, \text{ at } y = h(t) \quad (5)$$

$$\frac{\partial u}{\partial y} = 0, v = 0, \frac{\partial T}{\partial y} = 0, \frac{\partial C}{\partial y} = 0, \text{ at } y = 0 \quad (6)$$

where the wall of plates is indicated by temperature  $T_w$  and concentration  $C_w$ . Following Roseland approximation, the radiative heat flux is defined as [37]

$$q_r = \frac{-4\sigma^* \partial T^4}{3k_1^* \partial y} \quad (7)$$

where  $\sigma^*$  is the Stefan-Boltzmann constant and  $k_1^*$  is the mean absorption coefficient. It is assumed that the temperature differences within the flow are sufficiently small such that  $T^4$  can be expressed as linear function of temperature. Hence, expanding  $T^4$  in Taylor series about  $T_\infty$  and ignoring higher order terms lead to the following relation

$$T^4 \cong 4T_\infty^3 T - 3T_\infty^4 \quad (8)$$

Thus, substituting Eq. (7) and Eq. (8) into Eq. (3) yields

$$\begin{aligned} \frac{\partial T}{\partial t} + u \frac{\partial T}{\partial x} + v \frac{\partial T}{\partial y} = \alpha_f \left( 1 + \frac{16\sigma^* T_\infty^3}{3k_f k_1^*} \right) \frac{\partial^2 T}{\partial y^2} + \tau \left[ D_B \frac{\partial C}{\partial y} \frac{\partial T}{\partial y} + \frac{D_T}{T_\infty} \left( \frac{\partial T}{\partial y} \right)^2 \right] \\ + \frac{v_f}{c_f} \left( 1 + \frac{1}{\beta} \right) \left[ 4 \left( \frac{\partial u}{\partial x} \right)^2 + \left( \frac{\partial u}{\partial y} \right)^2 \right] + \frac{\sigma B^2(t)}{(\rho c)_f} u^2 + \frac{Q(t)}{(\rho c)_f} (T - T_\infty) \end{aligned} \quad (9)$$

The following similarity transformations adopted from Mustafa *et al.*, [24] and Ahmed *et al.*, [2] are introduced to reduce the nonlinear partial differential equations into the system of ordinary differential equations

$$u = \frac{\alpha x}{2(1 - \alpha t)} f'(\eta), \quad v = -\frac{\alpha l}{2\sqrt{(1 - \alpha t)}} f(\eta), \quad \eta = \frac{y}{l\sqrt{(1 - \alpha t)}}, \quad (10)$$

$$\theta = \frac{T - T_\infty}{T_w - T_\infty}, \quad \phi = \frac{C - C_\infty}{C_w - C_\infty},$$

where  $\eta$  is the local similarity variable,  $f(\eta)$ ,  $\theta(\eta)$  and  $\phi(\eta)$  are the dimensionless velocity, temperature and concentration of the fluid in the boundary layer region, respectively.

Using Eq. (10), the governing Eq. (2), Eq. (4) and Eq. (9) are converted to the following non-dimensional ordinary differential equations form

$$\left( 1 + \frac{1}{\beta} \right) f'''' - S(\eta f'''' + 3f'' + f'f'' - ff''') - Ha^2 f'' - \left( 1 + \frac{1}{\beta} \right) \frac{1}{Da} f'' = 0, \quad (11)$$

$$\begin{aligned} \frac{1}{Pr} \left( 1 + \frac{4}{3} Ra \right) \theta'' + S(f\theta' - \eta\theta' + \gamma\theta) + Ec \left[ \left( 1 + \frac{1}{\beta} \right) [(f'')^2 + 4\delta^2 (f')^2] + Ha^2 (f')^2 \right] \\ + N_b \phi' \theta' + N_t (\theta')^2 = 0, \end{aligned} \quad (12)$$

$$\frac{1}{Le} \phi'' + S(f\phi' - \eta\phi') + \frac{1}{Le N_b} \theta'' - R\phi = 0, \quad (13)$$

subject to the boundary conditions

$$f(\eta) = 0, f''(\eta) = 0, \theta'(\eta) = 0, \phi'(\eta) = 0, \quad \text{at } \eta = 0, \quad (14)$$

$$f(\eta) = 1, f'(\eta) = 0, \theta(\eta) = 1, \phi(\eta) = 0, \quad \text{at } \eta = 1. \quad (15)$$

The physical parameters involved in the above expressions,  $S$ ,  $Ha$ ,  $Da$ ,  $\delta$ ,  $Pr$ ,  $Ec$ ,  $R_d$ ,  $\gamma$ ,  $N_b$ ,  $N_t$ ,  $Le$  and  $R$  are the squeeze number, Hartmann number, Darcy number, dimensionless length, Prandtl number, Eckert number, radiation parameter, heat generation/absorption parameter, Brownian motion parameter, thermophoresis parameter, Lewis number and chemical reaction parameter, respectively, and are defined as

$$S = \frac{\alpha l^2}{2\nu_f}, \quad Ha = lB_0 \sqrt{\frac{\sigma}{\rho_f \nu_f}}, \quad Da = \frac{k_0}{\phi l^2}, \quad \delta = \frac{l}{x}(1 - \alpha t)^{1/2},$$

$$Pr = \frac{\nu_f}{\alpha_f}, \quad Ec = \frac{\alpha^2 x^2}{4c_f(T_H - T_\infty)(1 - \alpha t)^2}, \quad R_d = \frac{4\sigma^* T_\infty^3}{k_f k_1^*}, \quad \gamma = \frac{2Q_0}{\alpha(\rho c)_f},$$

$$N_b = \frac{\tau D_B(C_H - C_\infty)}{\nu_f}, \quad N_t = \frac{\tau D_T(T_H - T_\infty)}{\nu_f T_\infty}, \quad Le = \frac{\nu_f}{D_B}, \quad R = \frac{ak_2 l^2}{\nu_f}.$$

The physical quantities of interest which govern the flow such as local skin friction coefficient  $Cf_x$ , local Nusselt number  $Nu_x$  and local Sherwood number  $Sh_x$  are defined by Naduvinamani and Shanka [25] as follows

$$Cf_x = \frac{\tau_w}{\rho_f \nu_w^2}, \quad Nu_x = \frac{lq_w}{\alpha_f(T_H - T_\infty)}, \quad Sh_x = \frac{lq_s}{D_B(C_H - C_\infty)},$$

where  $\tau_w$ ,  $q_w$  and  $q_s$  are the wall skin friction, wall heat flux and wall mass flux, respectively, and are given by

$$\tau_w = \mu_B \left(1 + \frac{1}{\beta}\right) \left[\frac{\partial u}{\partial y}\right]_{y=h(t)}, \quad q_w = - \left( \left( \alpha_f + \frac{16\sigma^* T_\infty^3}{3(\rho c)_f k_1^*} \right) \frac{\partial T}{\partial y} \right)_{y=h(t)}, \quad q_s = -D_B \left( \frac{\partial C}{\partial y} \right)_{y=h(t)}.$$

The non-dimensional forms of the skin friction coefficient, Nusselt number and Sherwood number in terms of similarity variable are

$$\frac{l^2}{x^2}(1 - \alpha t)Re_x Cf_x = \left(1 + \frac{1}{\beta}\right) f''(1),$$

$$\sqrt{(1 - \alpha t)}Nu_x = - \left(1 + \frac{4}{3}R_d\right) \theta'(1),$$

$$\sqrt{(1 - \alpha t)}Sh_x = -\phi'(1),$$

where  $Re_x = \frac{xv_w}{\nu_f}$  is the local Reynolds number based on the squeezing velocity  $v_w$ .

### 3. Results and Discussion

The nonlinear ordinary differential Eq. (11) to Eq. (13) subject to boundary conditions Eq. (14) and Eq. (15) are solved numerically via Keller-box method. An algorithm is developed in MATLAB software in order to generate numerical and graphical solutions. Moreover, it is necessary to choose suitable guess for the step size  $\Delta\eta$  and boundary layer thickness  $\eta_\infty$ . In the present study,  $\Delta\eta = 0.01$  and  $\eta_\infty = 1$  are considered. The convergence criteria mainly refer to the relative difference between current and previous iterative values of velocity, temperature and concentration. The iteration process is terminated when all the values in  $\eta$  direction satisfy the convergence criteria  $10^{-5}$  [25].

In order to examine the physical behavior of velocity, temperature and concentration profiles, numerical computations are carried out for various values of squeeze number  $S$ , Casson fluid parameter  $\beta$ , Hartmann number  $Ha$ , radiation parameter  $R_d$ , heat generation or absorption parameter  $\gamma$ , Brownian motion parameter  $N_b$ , thermophoresis parameter  $N_t$  and chemical reaction parameter  $R$ . The present algorithm developed in MATLAB software are validated by comparing the numerical results with previous published works as limiting cases and presented in Table 1.

Table 1 displays the comparison of skin friction coefficient, Nusselt and Sherwood numbers for different values of  $S$  with the results of Mustafa *et al.*, [24] and Naduvinamani and Shanka [25]. The results showed an excellent agreement.

**Table 1**

Comparison of  $-f''(1)$ ,  $-\theta'(1)$  and  $-\phi'(1)$  for different values of  $S$  when  $\beta \rightarrow \infty$ ,  $Da \rightarrow \infty$  and  $Ha = R_d = \gamma = N_b = N_t = 0$

$S$	Mustafa <i>et al.</i> , [24]			Naduvamani and Shanka [25]			Present results		
	$-f''(1)$	$-\theta'(1)$	$-\phi'(1)$	$-f''(1)$	$-\theta'(1)$	$-\phi'(1)$	$-f''(1)$	$-\theta'(1)$	$-\phi'(1)$
-1.0	2.170090	3.319899	0.804558	2.170091	3.319899	0.804559	2.170255	3.319904	0.804558
-0.5	2.614038	3.129491	0.781402	2.617404	3.129491	0.781402	2.617512	3.129556	0.781404
0.01	3.007134	3.047092	0.761225	3.007134	3.047092	0.761225	3.007208	3.047166	0.761229
0.5	3.336449	3.026324	0.744224	3.336449	3.026324	0.744224	3.336504	3.026389	0.744229
2.0	4.167389	3.118551	0.701813	4.167389	3.118551	0.701813	4.167412	3.118564	0.701819

Figure 2 to 5 are plotted to analyse the dimensionless velocity, temperature and nanoparticles concentration profiles for effect of  $S$ . It is noteworthy here that  $S > 0$  represents the plates move away from each other and  $S < 0$  corresponds to the plates move towards each other. Figure 2 reveals that the component of normal velocity declines for increasing values of  $S > 0$  and the velocity increases for  $S < 0$  case. The increment in fluid velocity is due to the reason that the fluid pass through the channel at a faster rate when the plates move closer. Meanwhile, the velocity slow down as the fluid encounters more resistance when flowing in a wide channel (the plates move apart). The variation of  $S$  on axial velocity is displayed in Figure 3. It is found that fluid velocity reduces in the region  $0 \leq \eta < 0.45$  and it increases in the region  $0.45 < \eta \leq 1$  for  $S > 0$ . Also, the velocity rises in the region  $0 \leq \eta < 0.45$  and it decreases in the region  $0.45 < \eta \leq 1$  for  $S < 0$ . The cross-behavior of fluid flow is noticed on the centre of the channel. There is no significant effect of squeeze number on the velocity field at the critical point  $\eta_c = 0.45$ .

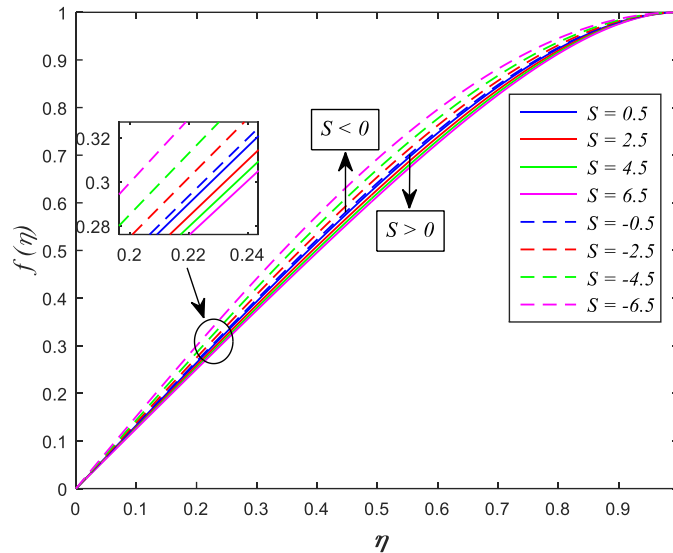


**Fig. 2.** Effect of  $S$  on radial velocity

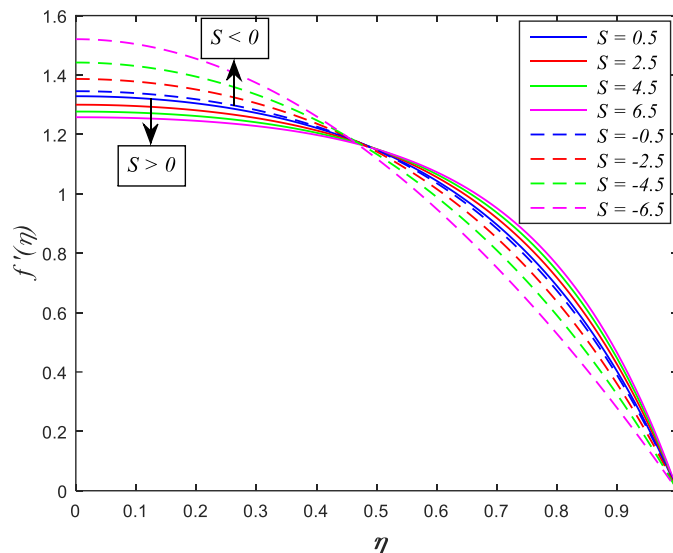


**Fig. 3.** Effect of  $S$  on axial velocity

The influence of  $S$  on temperature profile for both  $S > 0$  and  $S < 0$  cases is plotted in Figure 4. The fluid temperature drops for  $S > 0$  and rises for  $S < 0$ . The speed of fluid flow declines when the plates moves further, which cause the kinetic energy of fluid particles become weaker and consequently decreasing the temperature. It is stated that the kinetic energy is directly proportional to the temperature. Figure 5 depicts that increasing values of positive  $S$  enhance the nanoparticles concentration and it reduces for decreasing values of negative  $S$ . The squeeze number did not affect the concentration near the upper plate  $\eta = 1$ .



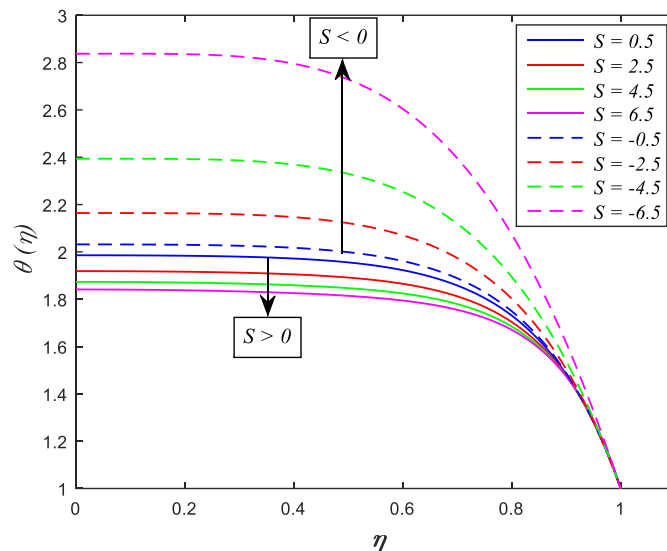


**Fig. 4.** Effect of  $S$  on temperature

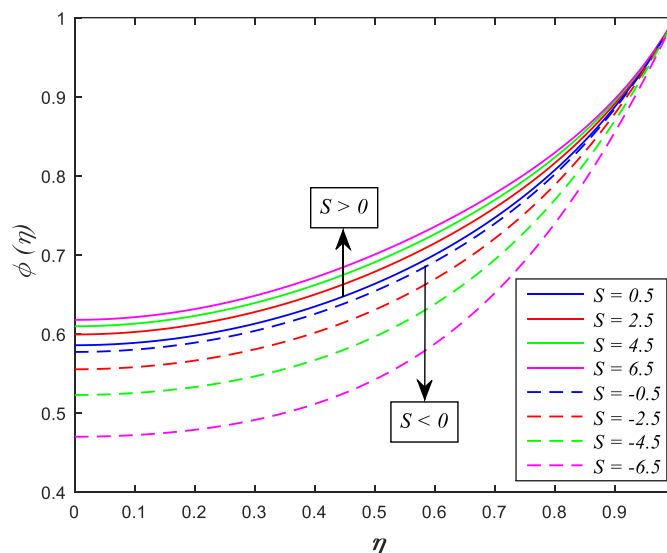


**Fig. 5.** Effect of  $S$  on nanoparticles concentration

The effect of  $\beta$  on the velocity, temperature and nanoparticles concentration profiles is presented in Figure 6 to Figure 9. It is noticed from Figure 6 that the normal velocity decelerates with increase in  $\beta$ . The reason behind this behavior is that higher values of  $\beta$  increase the viscosity of fluid, which offers more resistance to the fluid flow inside the channel. Figure 7 demonstrates that the axial velocity reduces in the region  $\eta < 0.5$  and it rises in the remaining region  $\eta > 0.5$  for increasing values of  $\beta$ . There is cross-behavior of fluid flow occurs at the centre region of the channel. The variation of temperature profile for different values of  $\beta$  is illustrated in Figure 8. It is observed that fluid temperature drops when  $\beta$  increases. This phenomenon indicates that increasing  $\beta$  cause enhancement in the modulus of elasticity of fluid. The reduction in the temperature is caused by larger modulus of elasticity, which results in thermal boundary layer becoming thinner. Figure 9 portrays that nanoparticles concentration is a decreasing function of  $\beta$ .

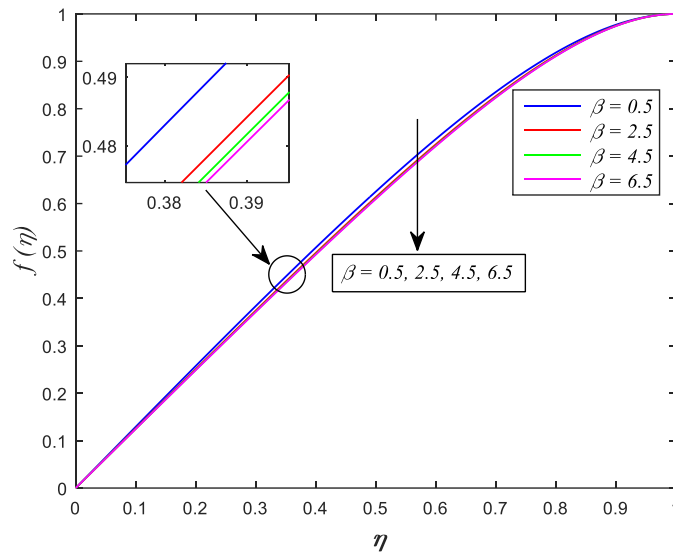


**Fig. 6.** Effect of  $\beta$  on radial velocity

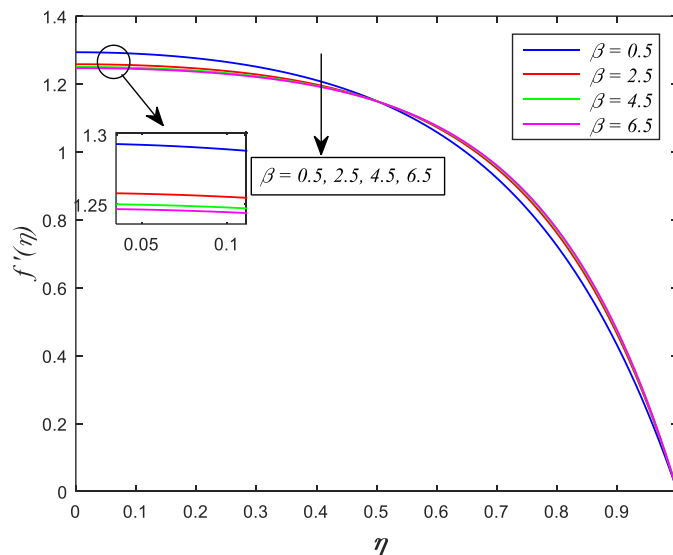


**Fig. 7.** Effect of  $\beta$  on axial velocity

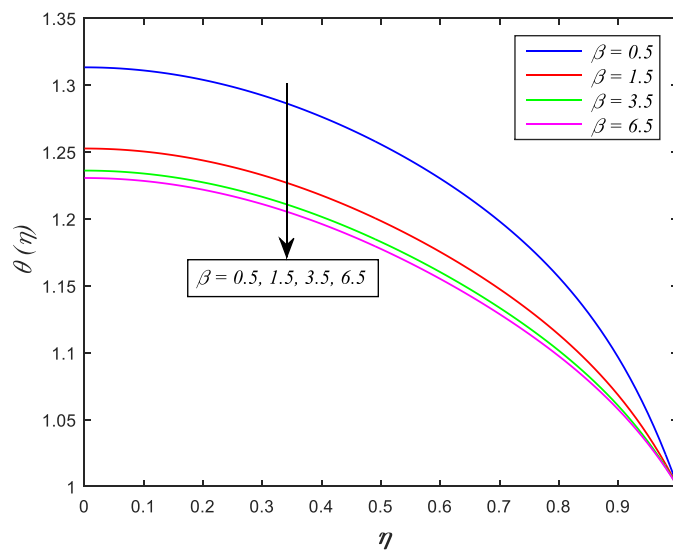


**Fig. 8.** Effect of  $\beta$  on temperature

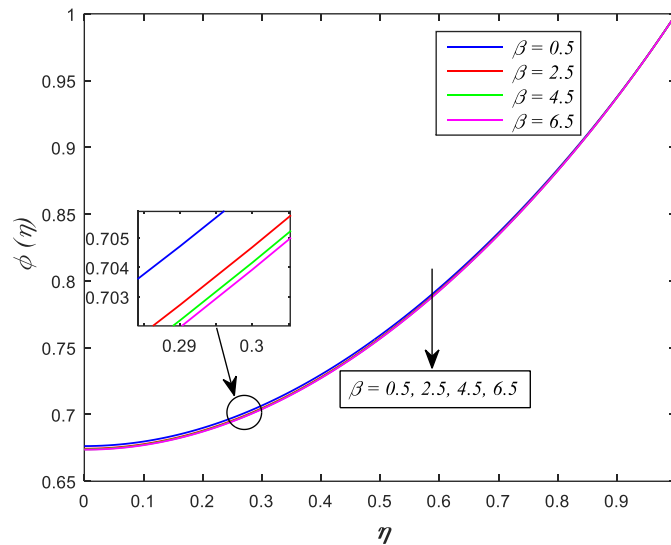


**Fig. 9.** Effect of  $\beta$  on nanoparticles concentration

Figure 10 to Figure 13 exhibit the influence of  $Ha$  on the velocity, temperature and nanoparticles concentration profiles. Figure 10 shows that increasing values of  $Ha$  reduce the normal velocity of fluid. A resistive-type force known as Lorentz force is generated due to an application of magnetic field in the electrically conducting fluid. This force presents resistance to the flow, which cause the fluid flow in the channel to slow down. It is clear from Figure 11 that the axial velocity declines in the region  $\eta < 0.5$  and rises in the other region  $\eta > 0.5$  when  $Ha$  increases. The midpoint of the channel is the centre of cross flow behavior. The variation of temperature profile for various values of  $Ha$  is portrayed in Figure 12. It is found that fluid temperature rises with increase in  $Ha$ . The presence of Joule and viscous dissipation in the energy equation also boosts the temperature. Figure 13 reveals that nanoparticles concentration decreases for increasing values of  $Ha$ .

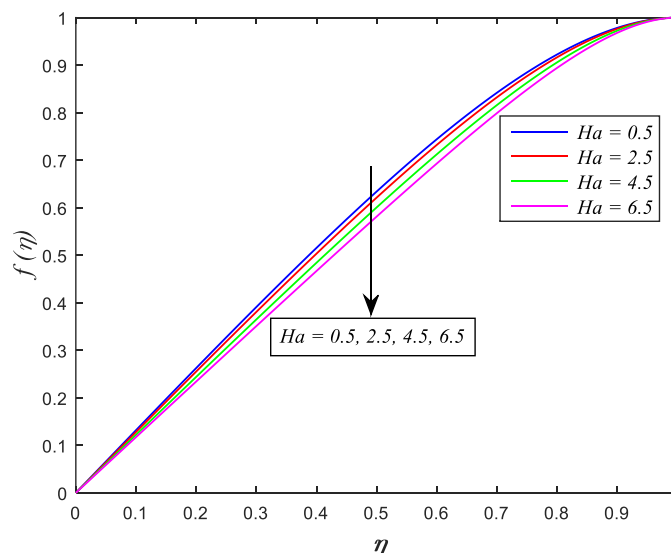


**Fig. 10.** Effect of  $Ha$  on radial velocity

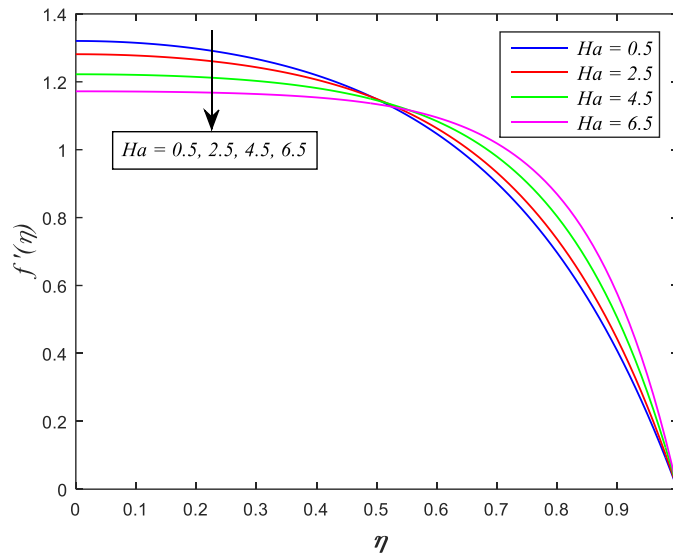


**Fig. 11.** Effect of  $Ha$  on axial velocity

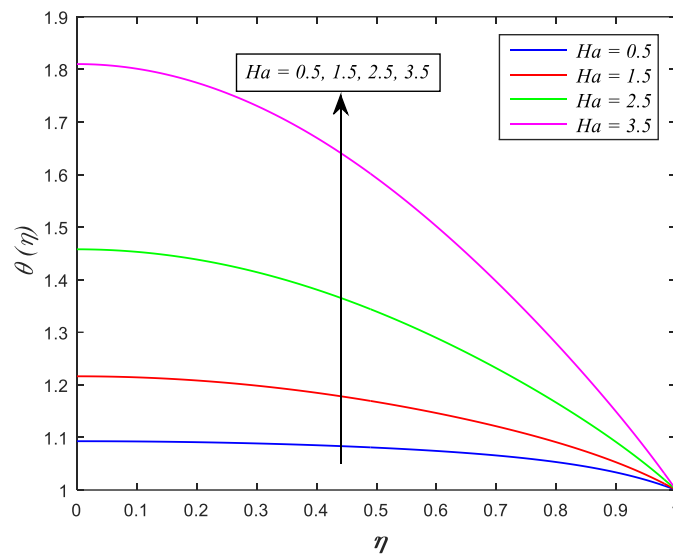


**Fig. 12.** Effect of  $Ha$  on temperature

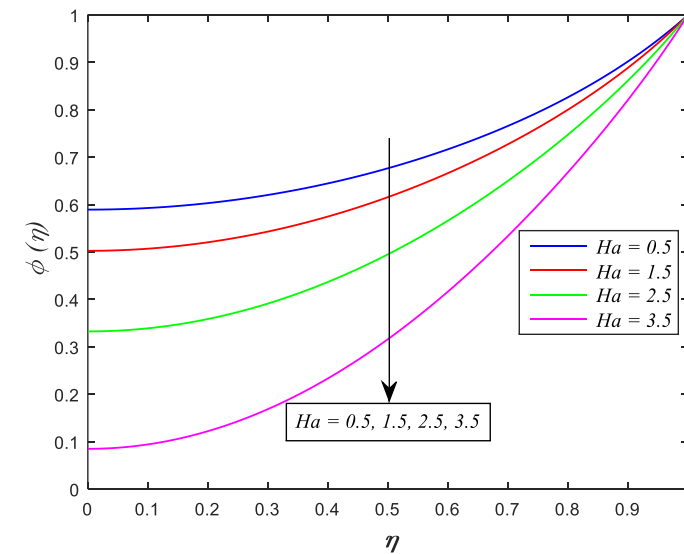


**Fig. 13.** Effect of  $Ha$  on nanoparticles concentration

The effect of  $R_d$  on temperature profile is depicted in Figure 14. It is noticed that the temperature of fluid drops as  $R_d$  increases. Figure 15 describes the influence of  $\gamma$  on temperature profile. It is noteworthy here that  $\gamma > 0$  and  $\gamma < 0$  represent heat generation and heat absorption case. It is observed that the temperature increases when  $\gamma > 0$  and decreases when  $\gamma < 0$ . The existence of heat source enhances the thermal energy of fluid and consequently raises the fluid temperature. The impact of  $N_b$  on temperature profile is shown in Figure 16. It is noticed that the temperature is an increasing function of  $N_b$ . It is due to the fact that Brownian motion of nanoparticles that occurs in nanofluid systems promotes the thermal conductivity of fluid. Therefore, increasing  $N_b$  elevates the heat transfer properties of nanofluid which results in enhancing fluid temperature. Figure 17 portrays the effect of  $N_t$  on temperature profile. It is found that the temperature rises slightly with increase in  $N_t$ . The reason is higher values of  $N_t$  indicates larger temperature gradient between fluid flow and hot plates. The presence of temperature difference induces the thermophoretic force on nanoparticles. The force boosts the disperse of nanoparticles from the hot plates to the fluid inside the channel which cause temperature increases in the flow region.

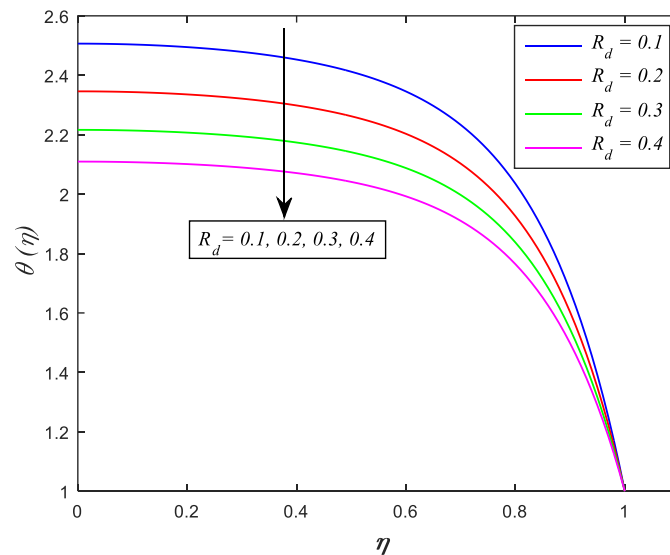


**Fig. 14.** Effect of  $R_d$  on temperature

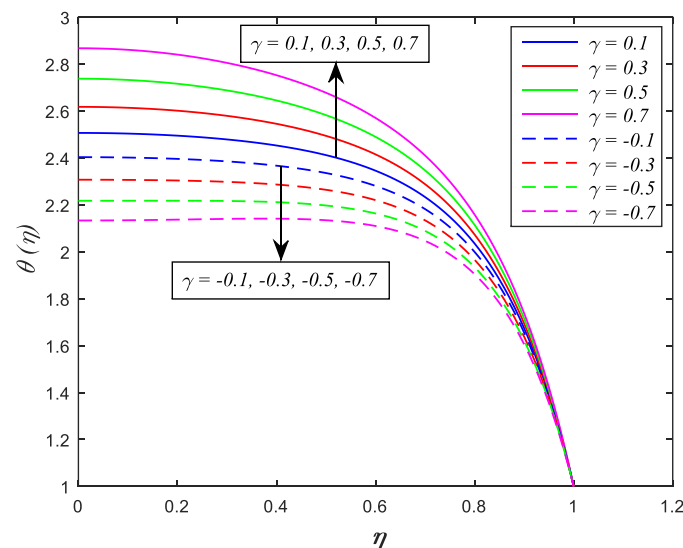


**Fig. 15.** Effect of  $\gamma$  on temperature

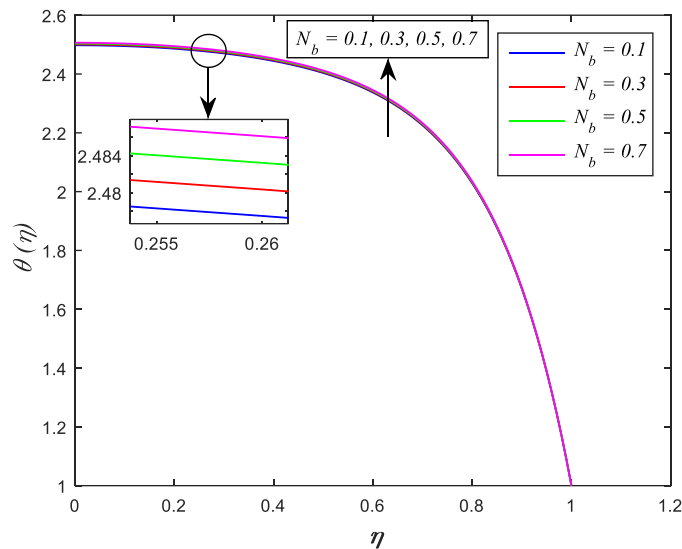


**Fig. 16.** Effect of  $N_b$  on temperature

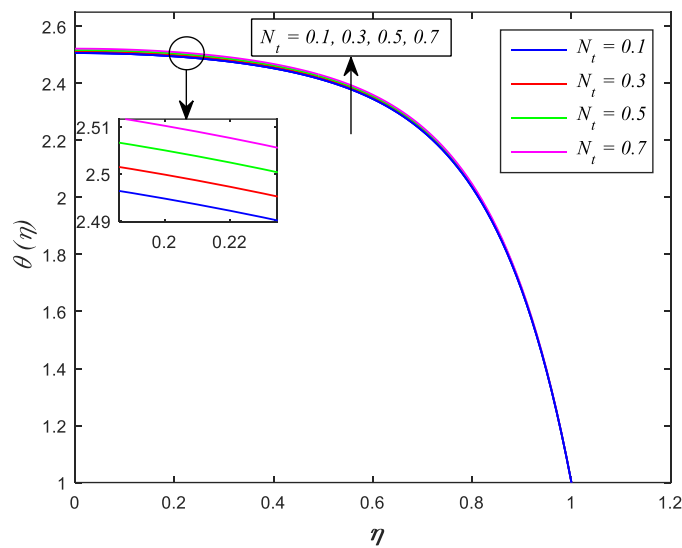


**Fig. 17.** Effect of  $N_t$  on temperature

The influence of  $N_b$  on concentration profile is exhibited in Figure 18. Clearly, nanoparticles concentration rises when values of  $N_b$  increases. It is important to note that the increment of random motion raise the kinetic energy of nanoparticles. The effective movement of nanoparticles from the plates to the moving fluid lead to enhancement in nanoparticles concentration. Figure 19 displays the impact of  $N_t$  on concentration profile. The larger values of  $N_t$  reduce the nanoparticles concentration. The thermophoretic force imposed on nanoparticles elevates the mass transfer from the moving fluid to the plates which results in decreasing nanoparticles concentration. The effect of  $R$  on concentration profile is demonstrated in Figure 20. It is observed that nanoparticles concentration declines in the case of destructive chemical reaction ( $R > 0$ ) and increases in the case of constructive chemical reaction ( $R < 0$ ). It is true with the fact that the mass transfer rate rises when  $R > 0$ , which cause reduction in nanoparticles concentration [24].

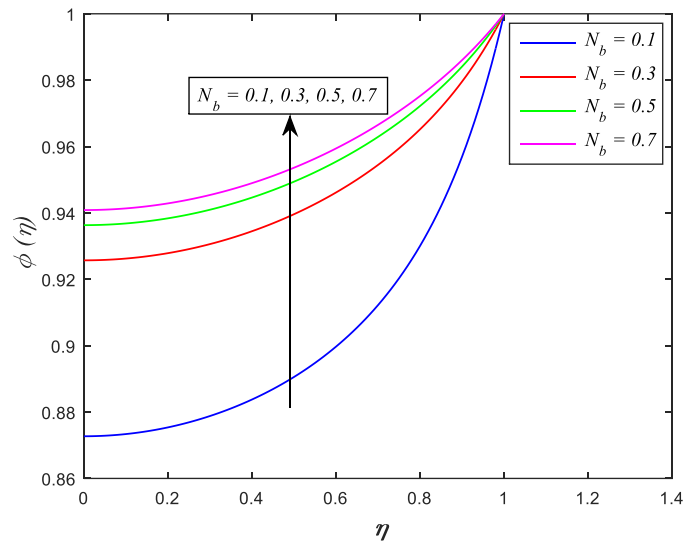


**Fig. 18.** Effect of  $N_b$  on nanoparticles concentration

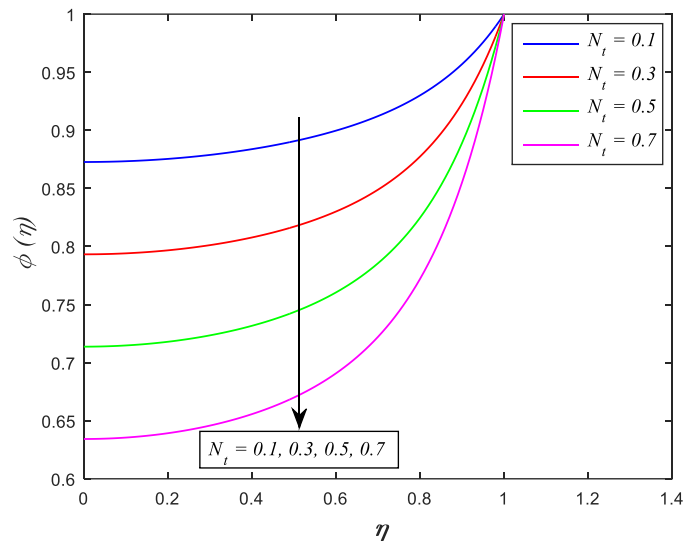


**Fig. 19.** Effect of  $N_t$  on nanoparticles concentration

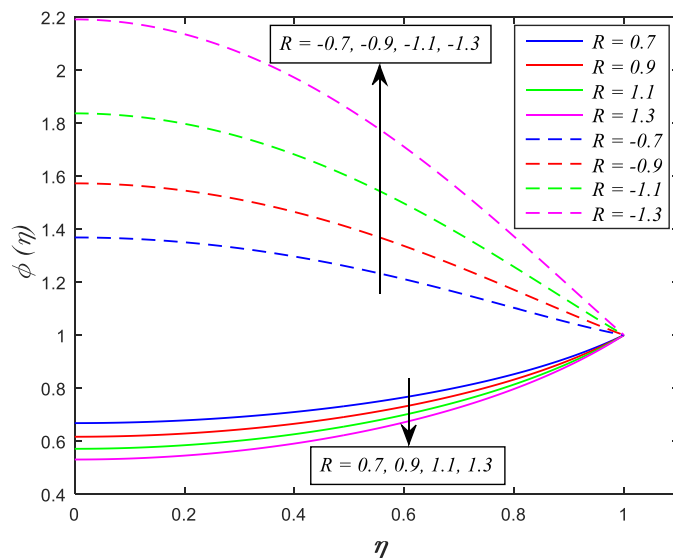


**Fig. 20.** Effect of  $R$  on nanoparticles concentration

#### 4. Conclusions

The heat and mass transfer characteristics of unsteady MHD flow of Casson nanofluid squeezing between two parallel plates saturated in a porous medium under the influence of chemical reaction, thermal radiation and heat generation or absorption was investigated numerically. The effects of viscous and Joule dissipation were also considered. The flow is induced by the motion of the upper plate towards or away from lower plate with an external velocity. The transformed governing equations are solved through Keller box method. The numerical solutions for skin friction coefficient, Nusselt and Sherwood numbers are validated with the previous works and excellent agreement is observed from both results. The effects of physical parameters, namely, squeeze number  $S$ , Casson fluid parameter  $\beta$ , Hartmann number  $Ha$ , radiation parameter  $R_d$ , heat generation/absorption parameter  $\gamma$ , Brownian motion parameter  $N_b$ , thermophoresis parameter  $N_t$  and chemical reaction parameter  $R$  on fluid velocity, temperature and concentration are analysed graphically. The main findings of this study can be summarized as follows

- i. The fluid velocity decelerates when the plates move apart ( $S > 0$ ) and it accelerates when the plates move closer ( $S < 0$ ).
- ii. The fluid velocity and nanoparticles concentration decrease with increase in  $Ha$ .
- iii. The fluid temperature drops for increasing values of  $R_d$ .
- iv. The fluid temperature enhances in the case of heat generation ( $\gamma > 0$ ) and it reduces in the case of heat absorption ( $\gamma < 0$ ).
- v. The increment of  $N_b$  boosts the fluid temperature and nanoparticles concentration.
- vi. The fluid temperature rises and nanoparticles concentration decreases when  $N_t$  increases.
- vii. The nanoparticles concentration declines for destructive chemical reaction ( $R > 0$ ) and it enhances for constructive chemical reaction ( $R < 0$ ).

#### Acknowledgement

The authors would like to acknowledge Ministry of Education (MOE) and Research Management Centre, Universiti Teknologi Malaysia (UTM) for financial support through vote number 07G77 for this research.

#### References

- [1] Acharya, Nilankush, Kalidas Das, and Prabir Kumar Kundu. "The squeezing flow of Cu-water and Cu-kerosene nanofluids between two parallel plates." *Alexandria Engineering Journal* 55, no. 2 (2016): 1177-1186. <https://doi.org/10.1016/j.aej.2016.03.039>
- [2] Ahmed, Naveed, Umar Khan, Sheikh Irfanullah Khan, Saima Bano, and Syed Tauseef Mohyud-Din. "Effects on magnetic field in squeezing flow of a Casson fluid between parallel plates." *Journal of King Saud University-Science* 29, no. 1 (2017): 119-125. <https://doi.org/10.1016/j.jksus.2015.03.006>
- [3] Alkasasbeh, Hamzeh T., Mohammed Z. Swalmeh, Abid Hussanan, and Mustafa Mamat. "Effects of mixed convection on methanol and kerosene oil based micropolar nanofluid containing oxide nanoparticles." *CFD Letters* 11, no. 1 (2019): 70-83.
- [4] Al-Saif, Abdul-Sattar JA, and Abeer Majeed Jasim. "A Novel Algorithm for Studying the Effects of Squeezing Flow of a Casson Fluid between Parallel Plates on Magnetic Field." *Journal of Applied Mathematics* 2019 (2019): 1-19. <https://doi.org/10.1155/2019/3679373>
- [5] Azimi Mohammadreza, and Riazi Rouzbeh. "MHD unsteady GO-water-squeezing nanofluid flow—heat and mass transfer between two infinite parallel moving plates: analytical investigation." *Sādhanā* 42, no. 3 (2017): 335-341. <https://doi.org/10.1007/s12046-017-0605-0>
- [6] Bujurke, N. M., Achar, P. K., and N. P. Pai. "Computer extended series solution for flow between squeezing plates." *Fluid Dynamics Research* 16, no. 2-3 (1995): 179-187. [https://doi.org/10.1016/0169-5983\(94\)00058-8](https://doi.org/10.1016/0169-5983(94)00058-8)



- [7] Buongiorno, J. "Convective transport in nanofluids." *Journal of heat transfer* 128, no. 3 (2006): 240-250.  
<https://doi.org/10.1115/1.2150834>
- [8] Cameron, Alastair, and C. M. Mc Ettles. "Basic lubrication theory." (1981).
- [9] Casson, N. "A flow equation for pigment-oil suspensions of the printing ink type." *Rheology of disperse systems* (1959).
- [10] Çelik, İbrahim. "Squeezing flow of nanofluids of Cu–water and kerosene between two parallel plates by Gegenbauer Wavelet Collocation method." *Engineering with Computers* (2019): 1-14.  
<https://doi.org/10.1007/s00366-019-00821-1>
- [11] Choi, Stephen US, and J. A. Eastman. "Enhancing thermal conductivity of fluids with nano-particles." *ASME, FED* 231 (1995): 99-105.
- [12] Dogonchi, A. S., K. Divsalar, and D. D. Ganji. "Flow and heat transfer of MHD nanofluid between parallel plates in the presence of thermal radiation." *Computer Methods in Applied Mechanics and Engineering* 310 (2016): 58-76.  
<https://doi.org/10.1016/j.cma.2016.07.003>
- [13] Eastman, Jeffrey A., S. U. S. Choi, Sheng Li, W. Yu, and L. J. Thompson. "Anomalously increased effective thermal conductivities of ethylene glycol-based nanofluids containing copper nanoparticles." *Applied physics letters* 78, no. 6 (2001): 718-720.  
<https://doi.org/10.1063/1.1341218>
- [14] Ghiasi, E. Khoshrouye, and Reza Saleh. "Analytical and numerical solutions to the 2D Sakiadis flow of Casson fluid with cross diffusion, inclined magnetic force, viscous dissipation and thermal radiation based on Buongiorno's mathematical model." *CFD Letters* 11, no. 1 (2019): 40-54.
- [15] Hedayati, Nima, and Abbas Ramiar. "Investigation of two phase unsteady nanofluid flow and heat transfer between moving parallel plates in the presence of the magnetic field using GM." *Transp Phenom Nano Micro Scales* 4, no. 2 (2016): 47-53.
- [16] Khan, Umar, Naveed Ahmed, Sheikh Irfanullah Khan, Zulfiqar Ali Zaidi, Yang Xiao-Jun, and Syed Tauseef Mohyud-Din. "On unsteady two-dimensional and axisymmetric squeezing flow between parallel plates." *Alexandria Engineering Journal* 53, no. 2 (2014): 463-468.  
<https://doi.org/10.1016/j.aej.2014.02.002>
- [17] Khan, Umar, Naveed Ahmed, S. I. U. Khan, Saima Bano, and Syed Tauseef Mohyud-Din. "Unsteady squeezing flow of a Casson fluid between parallel plates." *World Journal of Modelling and Simulation* 10, no. 4 (2014): 308-319.
- [18] Khan, Hamid, Mubashir Qayyum, Omar Khan, and Murtaza Ali. "Unsteady Squeezing Flow of Casson Fluid with Magnetohydrodynamic Effect and Passing through Porous Medium." *Mathematical Problems in Engineering* (2016).  
<https://doi.org/10.1155/2016/4293721>
- [19] Madaki, A. G., R. Roslan, M. Mohamed, and M. G. Kamardan. "Analytical solutions of squeezing unsteady nanofluid flow in the presence of thermal radiation." *Journal of Computer Science and Computational Mathematics* 6, no. 4 (2016): 451-463.
- [20] Madaki, A. G., R. Roslan, M. S. Rusiman, and C. S. K. Raju. "Analytical and numerical solutions of squeezing unsteady Cu and TiO<sub>2</sub>-nanofluid flow in the presence of thermal radiation and heat generation/absorption." *Alexandria Engineering Journal* 57, no. 2 (2018): 1033-1040.  
<https://doi.org/10.1016/j.aej.2017.02.011>
- [21] Maiga, Sidi El Becaye, Samy Joseph Palm, Cong Tam Nguyen, Gilles Roy, and Nicolas Galanis. "Heat transfer enhancement by using nanofluids in forced convection flows." *International journal of heat and fluid flow* 26, no. 4 (2005): 530-546.  
<https://doi.org/10.1016/j.ijheatfluidflow.2005.02.004>
- [22] Mittal, R. C., and Sapna Pandit. "Numerical simulation of unsteady squeezing nanofluid and heat flow between two parallel plates using wavelets." *International Journal of Thermal Sciences* 118 (2017): 410-422.  
<https://doi.org/10.1016/j.ijthermalsci.2017.04.019>
- [23] Muhammad, Sher, Syed Inayat Ali Shah, Gohar Ali, Mohammad Ishaq, Syed Asif Hussain, and Hidayat Ullah. "Squeezing nanofluid flow between two parallel plates under the influence of MHD and thermal radiation." *Asian Research Journal of Mathematics* 10, no. 1 (2018): 1-20.  
<https://doi.org/10.9734/ARJOM/2018/42092>
- [24] Mustafa, M., T. Hayat, and S. Obaidat. "On heat and mass transfer in the unsteady squeezing flow between parallel plates." *Meccanica* 47, no. 7 (2012): 1581-1589.  
<https://doi.org/10.1007/s11012-012-9536-3>
- [25] Naduvinamani, N. B., and Usha Shankar. "Radiative squeezing flow of unsteady magneto-hydrodynamic Casson fluid between two parallel plates." *Journal of Central South University* 26, no. 5 (2019): 1184-1204.  
<https://doi.org/10.1007/s11771-019-4080-0>

- [26] Pourmehran, O., M. Rahimi-Gorji, M. Gorji-Bandpy, and D. D. Ganji. "Analytical investigation of squeezing unsteady nanofluid flow between parallel plates by LSM and CM." *Alexandria Engineering Journal* 54, no. 1 (2015): 17-26.  
<https://doi.org/10.1016/j.aej.2014.11.002>
- [27] Rashidi, Mohammad Mehdi, Hamed Shahmohamadi, and Saeed Dinarvand. "Analytic approximate solutions for unsteady two-dimensional and axisymmetric squeezing flows between parallel plates." *Mathematical Problems in Engineering* (2008).  
<https://doi.org/10.1155/2008/935095>
- [28] Sampath, K. V. S., N. P. Pai, and K. Jacob. "A semi-numerical approach to unsteady squeezing flow of Casson fluid between two parallel plates." *Malaysian Journal of Mathematical Sciences* 12, no. 1 (2018): 35-47.
- [29] Sheikholeslami, M., and D. D. Ganji. "Heat transfer of Cu-water nanofluid flow between parallel plates." *Powder Technology* 235 (2013): 873-879.  
<https://doi.org/10.1016/j.powtec.2012.11.030>
- [30] Sheikholeslami, M., M. Hatami, and G. Domairry. "Numerical simulation of two phase unsteady nanofluid flow and heat transfer between parallel plates in presence of time dependent magnetic field." *Journal of the Taiwan Institute of Chemical Engineers* 46 (2015): 43-50.  
<https://doi.org/10.1016/j.jtice.2014.09.025>
- [31] Sheikholeslami, M., D. D. Ganji, and M. M. Rashidi. "Magnetic field effect on unsteady nanofluid flow and heat transfer using Buongiorno model." *Journal of Magnetism and Magnetic Materials* 416 (2016): 164-173.  
<https://doi.org/10.1016/j.jmmm.2016.05.026>
- [32] Siddiqui, Abdul M., Sania Irum, and Ali R. Ansari. "Unsteady squeezing flow of a viscous MHD fluid between parallel plates, a solution using the homotopy perturbation method." *Mathematical Modelling and Analysis* 13, no. 4 (2008): 565-576.  
<https://doi.org/10.3846/1392-6292.2008.13.565-576>
- [33] Sobamowo, M. G. "Magnetohydrodynamic squeezing flow of casson nanofluid between two parallel plates in a porous medium using method of matched asymptotic expansion." *Research on Engineering Structures and Materials* 4, no. 4 (2018): 257-277.  
<https://doi.org/10.17515/resm2017.46ds0315>
- [34] Sobamowo, Gbeminiyi, Lawrence Jayesimi, David Oke, Ahmed Yinusa, and Oluwatoyin Adedibu. "Unsteady Casson nanofluid squeezing flow between two parallel plates embedded in a porous medium under the influence of magnetic field." *Open J. Math. Sci.* 3, no. 1 (2019): 59-73.  
<https://doi.org/10.30538/oms2019.0049>
- [35] Stefan, M. "Experiments on apparent adhesion." *The London, Edinburgh, and Dublin Philosophical Magazine and Journal of Science* 47, no. 314 (1874): 465-466.  
<https://doi.org/10.1080/14786447408641062>
- [36] Sweet, Erik, K. Vajravelu, Robert A. Van Gorder, and I. Pop. "Analytical solution for the unsteady MHD flow of a viscous fluid between moving parallel plates." *Communications in Nonlinear Science and Numerical Simulation* 16, no. 1 (2011): 266-273.  
<https://doi.org/10.1016/j.cnsns.2010.03.019>
- [37] Ullah, Imran, Ilyas Khan, and Sharidan Shafie. "MHD natural convection flow of Casson nanofluid over nonlinearly stretching sheet through porous medium with chemical reaction and thermal radiation." *Nanoscale research letters* 11, no. 1 (2016): 527.  
<https://doi.org/10.1186/s11671-016-1745-6>
- [38] Wang, C-Y. "The squeezing of a fluid between two plates." *Journal of Applied Mechanics* 43, no. 4 (1976): 579-583.  
<https://doi.org/10.1115/1.3423935>
- [39] Xuan, Yimin, and Qiang Li. "Investigation on convective heat transfer and flow features of nanofluids." *Journal of Heat Transfer* 125, no. 1 (2003): 151-155.  
<https://doi.org/10.1115/1.1532008>
- [40] Que-zhong, X. I. E. "Model for effective thermal conductivity of nanofluids." *Applied Physics Letters* 307, no. 5 (2003): 313-317.  
[https://doi.org/10.1016/S0375-9601\(02\)01728-0](https://doi.org/10.1016/S0375-9601(02)01728-0)